Singular global components and frequency shift of the continuum GAMs in shaped tokamak plasmas

C. Wahlberg[1] and J. P. Graves[2]

[1]*Department of Physics and Astronomy, P.O. Box 516, Uppsala University, SE-751 20 Uppsala, Sweden;* [2]*Ecole Polytechnique Fédérale de Lausanne (EPFL), Swiss Plasma Center (SPC), CH-1015 Lausanne, Switzerland.*

Introduction Geodesic acoustic modes (GAMs) of a global character are frequently observed in tokamak plasmas. While many aspects of GAMs require a kinetic treatment, the MHD model offers a suitable framework for analytically studying various global aspects of these modes, including the global magnetic perturbations associated with the GAM [1]. Here we extend the analysis in [1] in order to study additional global aspects of GAMs. We show that the $m = 0$ and $m = 1$ components of the GAM eigenfunctions have singularities of type $(\psi - \psi_0)^{-1}$, where ψ is a flux function that labels the magnetic surfaces, and $\psi = \psi_0$ defines the singular surface [2]. These components extend from the plasma centre to the edge and are therefore both singular and of a global character. We also calculate the effects of a finite aspect ratio and a non-circular plasma cross section on the GAM frequency, and recover the dependence on inverse aspect ratio and Shafranov shift of the GAM frequency previously derived within gyrokinetic theory by Gao [3]. Furthermore, we show that there is a higher-order triangularity effect that, in addition to the previously known strong effect of elongation on the GAM frequency, also can be significant. The calculated triangularity effect predicts a nearly linearly increasing GAM frequency with increasing triangularity, a phenomenon observed also in TCV.

Plasma geometry We consider a toroidal plasma with large aspect ratio ($\varepsilon \sim r/R_0 \ll 1$) and non-circular cross section. We model the non-circularity in terms of the Fourier ellipticity $E(r)$ and Fourier triangularity $T(r)$ such that the shape of the flux surfaces is described by

$$\rho_s'(r, \omega') = r + E\cos 2\omega' + T\cos 3\omega' + \cdots \tag{1}$$

where (ρ', ω') is a local polar coordinate system with origin at the centre of the flux surface with radius r. We also consider the coefficients E and T to be of the same order of magnitude as the Shafranov shift Δ, i.e. $\Delta/r \sim E/r \sim T/r \sim \varepsilon$. In terms of the usual shaping parameters κ (elongation) and δ (triangularity) we have, to first order in ε, $\kappa = 1 - 2E/r$ and $\delta = 4T/r$. Extensions of these relations to second order in ε are derived in [4].

GAM eigenfunction The calculations are performed using a flux coordinate system (r, θ, φ) in which the plasma perturbation $\boldsymbol{\xi}$ and the perturbed magnetic field $\mathbf{Q}$ are represented by their contravariant components, i.e. $\boldsymbol{\xi} = \xi^i \mathbf{e}_i$ and $\mathbf{Q} = Q^i \mathbf{e}_i$. For a GAM eigenfunction expressed in terms of $\boldsymbol{\xi}$ and Q^φ, we include the leading-order $m = 0, 1, 2$ components in [1], the terms in [1] generated by the plasma non-circularity (denoted ξ_{NC} here), the component $\xi_0^{\theta(2)}$ (omitted

in [1]), plus the higher-order components $\xi_1^{r(3)}$, $\xi_1^{\theta(3)}$, $\xi_1^{\varphi(3)}$ and $Q_1^{\varphi(6)}$ [4]:

$$\xi^r = \varepsilon^2\xi_2^{r(2)}\sin 2\theta + \varepsilon^3\xi_{NC}^{r(3)} + \varepsilon^3\xi_1^{r(3)}\sin\theta \ldots \quad (2a)$$

$$\xi^\theta = \xi_0^{\theta(0)} + \varepsilon\xi_1^{\theta(1)}\cos\theta + \varepsilon^2\left(\xi_0^{\theta(2)} + \xi_2^{\theta(2)}\right)\cos 2\theta + \varepsilon^2\xi_{NC}^{\theta(2)} + \varepsilon^3\xi_1^{\theta(3)}\cos\theta + \cdots \quad (2b)$$

$$\xi^\varphi = \varepsilon\xi_1^{\varphi(1)}\cos\theta + \varepsilon^2\left(\xi_0^{\varphi(2)} + \xi_2^{\varphi(2)}\right)\cos 2\theta + \varepsilon^2\xi_{NC}^{\varphi(2)} + \varepsilon^3\xi_1^{\varphi(3)}\cos\theta + \cdots \quad (2c)$$

$$Q^\varphi = \varepsilon^4 Q_1^{\varphi(4)}\sin\theta + \varepsilon^5 Q_2^{\varphi(5)}\sin 2\theta + \varepsilon^5 Q_{NC}^{\varphi(5)} + \varepsilon^6 Q_1^{\varphi(6)}\sin\theta + \cdots \quad (2d)$$

The other two components of $\mathbf{Q}$ can be obtained from $Q^\theta = -J^{-1}\,\partial\left(JB^\theta\xi^r\right)/\partial r$ and $Q^r = B^\theta\,\partial\xi^r/\partial\theta$ [1]. The main purpose of the massive expansion above is to determine $\xi_0^{\theta(2)}$ and the shift of the GAM frequency from the sixth-order component $L_0^{(6)}$ in the expansion

$$L = \varepsilon^3 L_1^{(3)}\cos\theta + \varepsilon^4\textstyle\sum_{m=0-4} L_m^{(4)}\cos m\theta + \varepsilon^5\sum_{m=1-5} L_m^{(5)}\cos m\theta + \varepsilon^6 L_0^{(6)} + \cdots = 0 \quad (3)$$

where $L = \mathbf{e}_\theta\cdot[\rho\omega^2\boldsymbol{\xi} - \nabla(\delta P) + (\mathbf{B}\cdot\nabla)\mathbf{Q} + (\mathbf{Q}\cdot\nabla)\mathbf{B}]$, $\delta P = -\boldsymbol{\xi}\cdot\nabla p - \Gamma p(\nabla\cdot\boldsymbol{\xi}) + \mathbf{B}\cdot\mathbf{Q}$, $\mathbf{B}$ is the equilibrium magnetic field and p the equilibrium pressure.

After a computer-algebra calculation, employing a self-consistent equilibrium and similar expansions as Eq. (3) of the r- and φ-components of the equation of motion, and of the φ-component of the "frozen flux" equation, we obtain the following expression for $L_0^{(6)}$[4]:

$$L_0^{(6)} = \frac{\left[\omega_{GAM}^2(r)-\omega_{GAM}^2(r_0)\right]\rho\omega_{GAM}^2(r_0)r^2}{\omega_s^2\mu^2-\omega_{GAM}^2(r_0)}\tilde{\xi}_0^{\theta(2)} - \frac{r\rho\omega_s^2\omega_{GAM}^2(r_0)}{2\left[\omega_s^2\mu^2-\omega_{GAM}^2(r_0)\right]}\left(r\frac{d\tilde{\xi}_2^{r(2)}}{dr} + 3\tilde{\xi}_2^{r(2)}\right)$$

$$+\Xi(r,p,\mu,\Delta,E,T,\delta\omega^2)\xi_0^{\theta(0)}(r) \quad (4)$$

where $\omega_s^2 = \Gamma p(r)/\rho(r)R_0^2$, $\omega_{GAM}^2 = (2+\mu^2)\omega_s^2$ is the GAM frequency to lowest order in ε, $\mu \equiv q^{-1}$, and $\delta\omega^2$ denotes a second-order shift of the GAM frequency. Furthermore, the tilde notation in $\tilde{\xi}_0^{\theta(2)}$ and $\tilde{\xi}_2^{r(2)}$ indicates that these components exist *outside* the singular (GAM) surface, while the component $\xi_0^{\theta(0)}(r) = a\hat{\xi}\delta(r-r_0)$ only exists *at* $r = r_0$.

Singular GAM components Eq. (4) and the requirement that $L_0^{(6)} = 0$ outside $r = r_0$ gives

$$\tilde{\xi}_0^{\theta(2)}(r) = \frac{\omega_s^2(r)}{2r\left[\omega_{GAM}^2(r)-\omega_{GAM}^2(r_0)\right]}\left(r\frac{d\tilde{\xi}_2^{r(2)}}{dr} + 3\tilde{\xi}_2^{r(2)}\right) \quad (5)$$

Thus, if $d\omega_{GAM}^2/dr \neq 0$, $\tilde{\xi}_0^{\theta(2)}$ behaves like $(r-r_0)^{-1}$ [or like $(\psi-\psi_0)^{-1}$ if $d\psi/dr \neq 0$ at $r = r_0$], near $r = r_0$. In the calculation of $L_0^{(6)}$ in Eq. (4), $\xi_1^{\theta(3)}$, $\xi_1^{\varphi(3)}$ and $Q_1^{\varphi(6)}$ in Eq. (2) are also obtained. These components are also found to be singular near $r = r_0$, and can be expressed in terms of $\tilde{\xi}_0^{\theta(2)}$ as [4]: $\tilde{\xi}_1^{\varphi(3)} = (\mu r/R_0)\tilde{\xi}_0^{\theta(2)}$, $\tilde{\xi}_1^{\theta(3)} \cong (\mu^2 r/R_0)\tilde{\xi}_0^{\theta(2)}$ and $\tilde{Q}_1^{\varphi(6)} \cong -[r\rho\omega_{GAM}^2(r_0)/B_0]\tilde{\xi}_0^{\theta(2)}$. As a consequence, the characteristic $m = 0$ and $m = 1$ flow pattern of the GAM existing *at* the singular surface also exists in the form of an *identical flow pattern*

consisting of the singular components above *outside the singular surface*. The existence of these singular components outside $r = r_0$ gives the characteristic $m = 0$ and $m = 1$ components of the "eigenfunction" of a continuum GAM a finite radial extension and a global character, illustrated in Fig. 1 with the profiles of $r\tilde{\xi}_0^{\theta(2)}$ $(m = 0)$, $R_0\tilde{\xi}_1^{\varphi(3)}(m = 1)$, $R_0\left(\nabla\cdot\tilde{\boldsymbol{\xi}}\right)_1^{(3)}$ $(m = 1)$ (related to the density and pressure fluctuations), as well as the radial profile of $\tilde{\xi}_2^{r(2)}$ $(m = 2)$. The q-profile is given by $q(r) = 1 + 3(r/a)^4$ and $r_0 = 0.7a$. In addition to the singularity $(r - r_0)^{-1}$ of the tangential components of $\tilde{\boldsymbol{\xi}}$, the normal component $\tilde{\xi}^r$ has a logarithmic singularity at $r = r_0$ [2, 4], illustrated by the dotted curves in the figure.

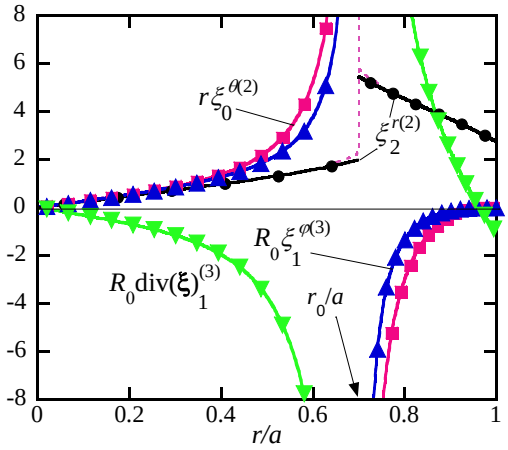

Fig. 1. Singular $m = 0$, $m = 1$ and $m = 2$ components of a continuum GAM with the singular surface at $r_0 = 0.7a$.

Shift of the GAM frequency Since $L_0^{(6)}$ has to be zero also *at* $r = r_0$ it follows from Eq. (4) that we must have $\Xi = 0$ at $r = r_0$. This determines the shift of the GAM frequency induced by finite aspect ratio, ellipticity and triangularity. Including the full dependence on $q \equiv \mu^{-1}$ it turns out that $\Xi = 0$ leads to the following, modified GAM frequency [4]

$$\frac{\omega_{GAM}^2}{\tilde{\omega}_{GAM}^2} = 1 + \frac{1}{\mu^2+2}\left(\frac{dE}{dr} + \frac{3E}{r}\right) + \left[\frac{\Delta'}{3\mu^2-2} + \frac{r(\mu^4+\mu^2+6)}{6R_0(\mu^2+2)^2} + \frac{4r\mu^2(\mu^2-2)}{3R_0(\mu^2+2)^2(3\mu^2-2)}\right]\left(\frac{dT}{dr} + \frac{4T}{r}\right)$$

$$- \frac{(15\mu^2-2)(\Delta')^2}{2(\mu^2+2)(3\mu^2-2)} + \frac{r(15\mu^4+9\mu^2-10)\Delta'}{2R_0(\mu^2+2)(3\mu^2-2)} - \frac{r^2(12\mu^6+5\mu^4+28\mu^2-24)}{4R_0^2(\mu^2+2)(3\mu^2-2)} - \frac{\beta^*(r)(4\mu^2+1)}{4\mu^2}$$

$$- \frac{2\mu^2}{3(\mu^2+2)(3\mu^2-2)}\left(\frac{dT}{dr} + \frac{4T}{r}\right)^2 - \frac{40\mu^2}{3(\mu^2+2)(15\mu^2-2)}\left(\frac{dT}{dr} - \frac{2T}{r}\right)^2 - \frac{9\mu^2}{2(\mu^2+2)(4\mu^2-1)}\left(\frac{dE}{dr} - \frac{E}{r}\right)^2 \quad (6)$$

where $\beta^* = \Gamma p/B_0^2$ and $\tilde{\omega}_{GAM}^2 = [\Gamma p/\rho(R_0 + \Delta)^2](2 + 1/q^2)$. Expressing E and T in terms of κ and δ, assuming that $q \gg 1$, and neglecting the β^*-term as well as the nonlinear terms in E and T, the following, simplified version of Eq. (6) can be derived [4]

$$\frac{\omega_{GAM}^2}{2c_s^2/R^2} \cong 1 - 2\frac{\kappa-1}{\kappa+1} - \frac{r\kappa'}{(\kappa+1)^2} + \left(\frac{r}{16R_0} - \frac{\Delta'}{8}\right)\left[6\delta + r^2\left(\frac{\delta}{r}\right)'\right] - \left(1 - \frac{6.5}{q^2}\right)\frac{(\Delta')^2}{4} + \frac{5r\Delta'}{4R_0} - \frac{3}{2}\left(\frac{r}{R_0}\right)^2$$

$$+\chi_0(r)\delta_a^2 \quad (7)$$

where δ_a is the edge triangularity and $\chi_0(r)$ depends on the q-profile [4]. For a plasma with circular cross section, the frequency shift $\delta\omega_{GAM}$ due to a finite aspect ratio that one obtains from Eq. (7) reproduces, in the limit $q \to \infty$, the frequency shift derived by Gao using gyrokinetic theory [3].

Fig. 2(a) shows ω_{GAM} vs δ_a including the effect of beta (and associated Shafranov shift Δ'). The solid curves in this figure are based on the full Eq. (6) while the dashed curves are obtained from Eq. (7). Other parameters in this figure are $\kappa_a = 1.3$, $\varepsilon_a = 0.2$, $q(r) = 1 + 3(r/a)^2$,

$r_0/a = 0.95$ and $p(r) = p_0[1-(r/a)^2]^2$. A corresponding, experimental scan of f_{GAM} vs δ in the TCV tokamak is shown in Fig. 2(b). The discharges used for this plot are similar to those described by Huang *et al*. [5], where the scan in triangularity was obtained while trying to keep all other relevant parameters constant (as constant as possible).

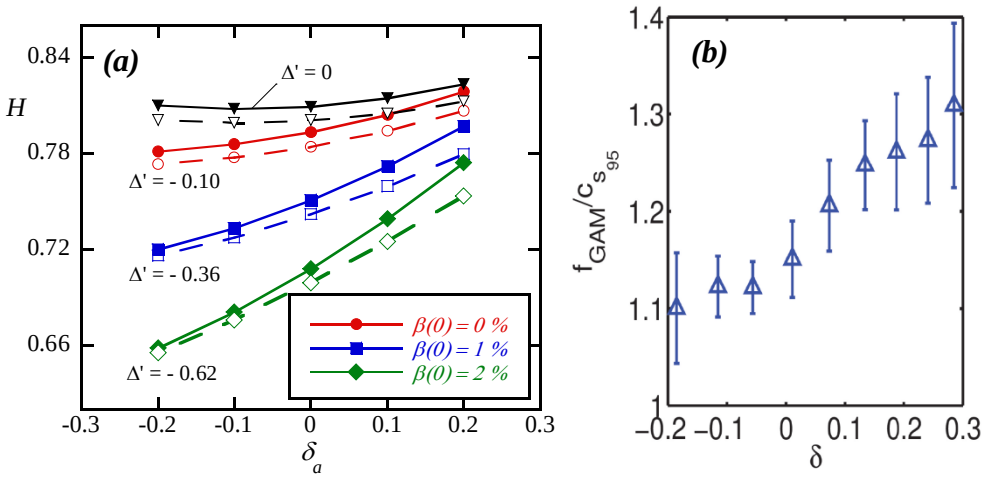

Fig. 2. ***(a)*** *Dependence of the GAM frequency on δ_a and $\beta(0)$, calculated from Eq. (6). $H \equiv \omega_{GAM}/\tilde{\omega}_{GAM}$, $\kappa_a = 1.3$, $\varepsilon_a = 0.2$, $q(r) = 1 + 3(r/a)^2$ and $r_0/a = 0.95$. The dashed curves are calculated from Eq. (7).* ***(b)*** *GAM frequency vs edge triangularity measured in TCV (courtesy of Z. Huang and S. Coda).*

Conclusions The individual "eigenmodes" of the GAM continuum in tokamaks have much broader radial profiles than what has been known previously. The reason is that the GAM eigenmodes include global $m = 0$ and $m = 1$ components of the plasma flow, and global components of the density and pressure perturbations (also with $m = 1$) that have singularities of type $(r - r_0)^{-1}$ near the GAM surface (see Fig.1). In this respect, the GAM eigenmodes have similar properties as all other eigenmodes in the continuous MHD spectrum of axisymmetric, toroidal plasmas [2]. It is possible [4] that this globality of the $m = 0$ and $m = 1$ components of a single continuum GAM may have something to do with the "GAM eigenmodes" detected in several tokamaks. Another result we obtain from the same calculation is the shift of the GAM frequency due to a finite aspect ratio (including the effect of the Shafranov shift derivative Δ'), and due to a non-circular plasma cross section. We find, in particular, a triangularity effect that predicts a nearly linearly increasing GAM frequency with increasing triangularity, a phenomenon observed also in TCV. A comparison is shown in Fig. 2, and a remarkably similar dependence is seen in the analytic triangularity prediction and the experimental data.

Acknowledgements Many thanks to Dr. Z. Huang, Dr. S. Coda and the TCV team for the TCV GAM data shown in Fig. 2(b) and for useful discussions. This work was supported in part by the Swiss National Science Foundation.

References

[1] C Wahlberg and J P Graves, Plasma Phys. Control. Fusion **58**, 075014, 2016.
[2] Y. P. Pao, Nucl. Fusion **15**, 631, 1975.
[3] Z. Gao, Physics of Plasmas **17**, 092503, 2010.
[4] C Wahlberg and J P Graves, Plasma Phys. Control. Fusion **61**, 075013, 2019.
[5] Z. Huang, S. Coda and the TCV team, Plasma Phys. Control. Fusion **61,** 014021, 2018.